

On Event-Based Sampling for \mathcal{H}_2 -Optimal Control

Marcus Thelander Andrén, Bo Bernhardsson, Anton Cervin and Kristian Soltesz

Abstract—We consider the problem of finding an event-based sampling scheme that optimizes the trade-off between sampling rate and \mathcal{H}_2 performance of a linear time-invariant system driven by white noise. We base our analysis on a recently presented sampled-data controller structure, which has been proven to be \mathcal{H}_2 -optimal for any given sampling sequence. We show that optimization of the sampling scheme is related to an elliptic convection-diffusion type partial differential equation over a domain with free boundary, a so called Stefan problem. A closed form of the optimal sampling scheme is presented for the multidimensional integrator case, together with a numerical method for obtaining it in the second order general case. In the integrator case, we prove that the optimal event-based sampling scheme will always outperform periodic sampling, and present tight bounds on the improvement. Also, we give numerical examples demonstrating the performance improvement for both the integrator case and a more general case.

Index Terms—Event-based sampling, \mathcal{H}_2 -optimal control, sampled-data control, linear reset systems

I. INTRODUCTION

Sampled-data control has a long history of implementation using zero-order hold (ZOH) actuation and periodic sampling, with a well-established theoretical framework [1]. However, in areas where sampling and/or actuation is costly, e.g., due to constraints on network bandwidth and computational power, the question arises whether a more efficient use of resources is possible. This is where the field of event-based control has emerged, where sampling and actuation are triggered only when controlled variables deviate significantly from their current setpoints. Early pioneering work in [2] and [3] demonstrated the potential of event-based control, and it has since been a field of much activity [4]–[7].

In event-based control, both the inter-sample behavior of the control signal and the sampling scheme are considered parts of the design problem. For a closed-loop system of the form in Fig. 1, this corresponds to co-design of the sampler \mathcal{S} , the hold \mathcal{H} , the discrete-time controller \bar{K} and the sequence of sampling instants $\{t_i\}_{i \in \mathbb{N}}$. This co-design problem has traditionally been seen as a difficult task, but recently a \mathcal{H}_2 -optimal solution has been presented for linear time-invariant (LTI) systems in [8], [9]. Furthermore, the \mathcal{H}_2 -optimal sampled-data controller structure is shown to be optimal for any uniformly bounded sampling sequence. This implies that the co-design problem is separable, and that the remaining problem is to find the sampling scheme which gives the optimal \mathcal{H}_2 performance for a given cost on

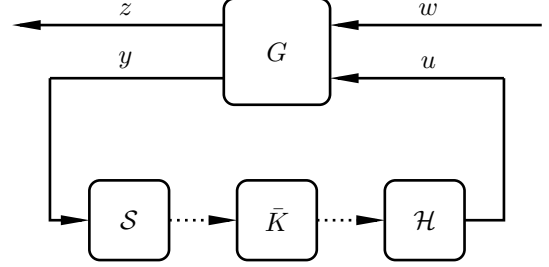


Fig. 1. An LTI system G in feedback with a sampled-data controller consisting of a sampler \mathcal{S} , a hold \mathcal{H} and a discrete-time controller \bar{K} . Solid lines represent continuous-time signals, whereas dashed lines represent discrete-time signals.

sampling effort, e.g., the average sampling rate. In the setup we consider in Fig. 1, the sampling effort represents costly data transmission from the sensor side to the actuator side.

The results in [8], [9] also show that the \mathcal{H}_2 performance is governed by a linear reset system. Reset systems in event-based control have been considered in several works, e.g. [2], [10], [11], and the results in [8], [9] confirm that they play a fundamental role. In [11, Paper I & II], a general framework for optimal event-based impulse control is developed, and we show that this framework can in fact be directly applied for solving the optimal sampling problem.

The contribution of this paper is to derive the optimal event-based sampling scheme for the controller structure in [8], [9] using the framework in [11]. We show that the optimal sampling problem is equivalent to solving a stationary partial-differential equation (PDE) with free boundary and present a closed-form solution for the n -dimensional integrator case. The performance ratio between periodic and optimal event-based sampling for this system is shown to lie in the interval $[1 + \frac{2}{n}, 3]$. For the general case, we describe a method for obtaining the optimal sampling scheme numerically. Finally, the method is applied to two second-order example systems.

II. PROBLEM FORMULATION

We consider the problem of finding the optimal sampling scheme for the closed-loop system in Fig. 1. Here, G is a continuous-time LTI system, which is assumed to have a realization of the form

$$G : \begin{cases} \dot{x}(t) = Ax(t) + B_w w(t) + B_u u(t), \\ z(t) = C_z x(t) + D_{zu} u(t), \\ y(t) = C_y x(t) + D_{yw} w(t), \end{cases} \quad (1)$$

satisfying the standard assumptions for the output feedback \mathcal{H}_2 problem in [12, Sec. 14.5]. The system G is driven by the

control signal u and the unit-intensity white noise w (scaling and reshaping of the noise spectrum can always be included as a noise model in G). The outputs are the measurement y and controlled signal z .

We use the asymptotic variance of z as a performance measure, which can also be seen as the squared \mathcal{H}_2 -norm of the closed-loop system $T_{zw} : w \rightarrow z$ in this stochastic setting:

$$\|T_{zw}\|_2^2 := \lim_{T \rightarrow \infty} \frac{1}{T} \int_0^T \text{Tr}(\mathbb{E}[z(t)z(t)^\top]) dt. \quad (2)$$

The average sampling rate of the system is defined as

$$f := \lim_{T \rightarrow \infty} \frac{1}{T} N_{[0,T]}, \quad (3)$$

where $N_{[0,T]}$ is the expected number of samples in the interval $[0, T]$. We then define the objective of finding the optimal sampling scheme as

$$\min_{\{t_i\}} J = \min_{\{t_i\}} \|T_{zw}\|_2^2 + \rho f, \quad (4)$$

where ρ is the per-sample cost, which decides the optimal trade-off between sampling rate and performance. The optimization (4) is performed over the sampling sequence $\{t_i\}$, which is based on knowledge of $y(t)$ for $t \in [0, t_i]$ alone.

We consider the sampled-data controller structure $K = S\bar{K}\mathcal{H}$ fixed to the \mathcal{H}_2 -optimal structure from [8], [9], which is proven to be optimal for any uniformly bounded sampling sequence $\{t_i\}^1$. This controller structure will be reviewed next.

A. The \mathcal{H}_2 -Optimal Controller Structure

With no restrictions on sampling, the controller minimizing $\|T_{zw}\|_2^2$ for the system (1) is the continuous-time LQG controller [12, Ch. 14], with the realization

$$\begin{cases} \dot{\hat{x}}(t) &= (A + B_u F + L C_y) \hat{x}(t) - L y(t), \\ u(t) &= F \hat{x}(t), \end{cases} \quad (5)$$

where F and L solve the two algebraic Riccati equations

$$\begin{cases} A^\top X + X A + C_z^\top C_z - F^\top (D_{zu}^\top D_{zu}) F = 0, \\ F = -(D_{zu}^\top D_{zu})^{-1} (B_u^\top X + D_{zu}^\top C_z), \\ A Y + Y A^\top + B_w B_w^\top - L (D_{yw} D_{yw}^\top) L^\top = 0, \\ L = -(Y C_y^\top + B_w D_{yw}^\top) (D_{yw} D_{yw}^\top)^{-1}. \end{cases}$$

The minimum cost $\gamma_0^2 := \min \|T_{zw}\|_2^2$ is then [12, Thm. 14.7]

$$\gamma_0^2 = \text{Tr}(B_w^\top X B_w) + \text{Tr}(C_z Y C_z^\top) + \text{Tr}(X A Y + Y A^\top X). \quad (6)$$

Since sampling will always lead to some performance degradation, (6) is the lower bound on $\|T_{zw}\|_2^2$ for any sampled-data controller structure K . The \mathcal{H}_2 -optimal sampled-data controller structure is given by the following theorem:

¹While a deterministic setting is considered in [8], [9], the same results also hold for the current stochastic setting. This is formally proven in [13].

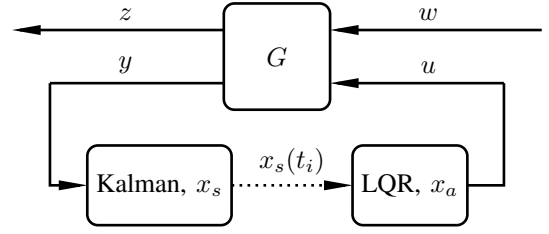


Fig. 2. A realization of the \mathcal{H}_2 -optimal sampled-data controller structure, which has a Kalman–Bucy filter on the sensor side, which intermittently transmits its estimate to an LQR controller simulating the closed-loop system on the actuator side.

Theorem 1 ([9, Thm. 3]): The optimal achievable performance for the system in Fig. 1 among all causal sampled-data controllers K for any uniformly bounded sampling sequence $\{t_i\}$ is

$$\min \|T_{zw}\|_2^2 = \gamma_0^2 + \|H\|_2^2, \quad (7)$$

where H is a linear reset system with realization

$$H : \begin{cases} \dot{x}_h(t) &= A x_h(t) + L \epsilon, & x_h(t_i) &= 0, \\ \eta(t) &= (D_{zu}^\top D_{zu})^{\frac{1}{2}} F x_h(t). \end{cases} \quad (8)$$

The input $\epsilon = y - C_y x_s$ is the innovations signal of the Kalman–Bucy filter

$$\dot{x}_s(t) = A x_s(t) + B_u u(t) - L(y(t) - C_y x_s(t)), \quad (9)$$

operating on the sensor side measurement y . Furthermore, $x_h = x_a - x_s$, where x_a is the state vector of an intermittently reset LQR controller simulating the closed loop on the actuator side

$$\begin{aligned} \dot{x}_a(t) &= (A + B_u F) x_a(t), & x_a(t_i) &= x_s(t_i), \\ u(t) &= F x_a(t). \end{aligned} \quad (10)$$

Proof: See proof of Theorem 3 in [9]. ■

Remark 1: The \mathcal{H}_2 -optimal controller structure also has a representation given explicitly in \mathcal{S} , \bar{K} and \mathcal{H} , presented in [9]. It would be considered for practical implementations, but is less intuitive for analysis.

A block diagram of the optimal controller structure (9), (10) from Theorem 1 is presented in Fig. 2. Naturally, a copy of (10) should be featured on the sensor side to avoid an analog channel from the actuator to the sensor.

The system H from Theorem 1 describes the inter-sample degradation compared to the continuous-time LQG performance. It is driven by the innovations signal ϵ , which, with the assumption on w , will be a white process with intensity $D_{yw} D_{yw}^\top$ (see e.g [14, Ch. 8, Thm 6.3]).

B. The Optimal Sampling Problem

With Theorem 1, we can use (7) to re-formulate the original problem (4) as

$$\min_{\{t_i\}} J = \gamma_0^2 + \min_{\{t_i\}} J_H, \quad (11)$$

$$J_H := \|H\|_2^2 + \rho f. \quad (12)$$

I.e., it is sufficient to consider optimization over J_H . With knowledge of y , we construct a sampling scheme based

directly on x_h using (9), (10). Denote this scheme $\phi(x_h) : x_h \rightarrow \{0, 1\}$, where 1 denotes “sample” and 0 denotes “no sample”, i.e., $\{t_i\} = \{t | \phi(x_h(t)) = 1\}$. The problem of finding the optimal sampling scheme is reformulated as

$$\begin{aligned} \min_{\phi(x_h(t))} \quad & J_h, \\ \text{s.t.} \quad & \dot{x}_h(t) = Ax_h(t) + e(t), \\ & x_h(t_i) = 0, \end{aligned} \quad (13)$$

where $e = L\epsilon$ is a white process with intensity $R = LD_{yw}D_{yw}^\top L^\top$.

III. A FRAMEWORK FOR THE OPTIMAL SAMPLING PROBLEM

A problem similar to (13) was considered in [11, Paper I and II], and we will build on the framework presented there. The framework considers optimal event-based impulse control of LTI systems, driven by white noise, where the system state is reset to zero at each actuation. The cost function used in [11] is of the form

$$J_i = \lim_{T \rightarrow \infty} \frac{1}{T} \mathbb{E} \left[\int_0^T x^\top(t) Q x(t) dt \right] + \rho f,$$

with f and ρ defined as in (3), (4). The matrix Q is considered a design variable. Note that J_h is equivalent to J_i since

$$\|H\|_2^2 = \lim_{T \rightarrow \infty} \frac{1}{T} \mathbb{E} \left[\int_0^T x_h^\top(t) \underbrace{F^\top D_{zu}^\top D_{zu} F}_Q x_h(t) dt \right],$$

i.e., we consider $Q = F^\top D_{zu}^\top D_{zu} F$. The framework of [11, Paper I and II] is thus directly applicable to (13).

A. The Equivalent Value Function Problem

The framework in [11, Paper I and II] is based on introducing and optimizing bounds on the cost, $\underline{J} \leq J_h \leq \bar{J}$. The bounds are shown by finding a bounded, \mathcal{C}^2 value function $V : x_h \rightarrow \mathbb{R}$, satisfying the path constraints

$$\begin{cases} \frac{1}{T}(j + \mathbb{E}[V(x_h(T)) - V(x_h(0))]) \geq \underline{J}, \\ \frac{1}{T}(j + \mathbb{E}[V(x_h(T)) - V(x_h(0))]) \leq \bar{J}, \end{cases}$$

$$j =: \mathbb{E} \left[\int_0^T x^\top(t) Q x(t) dt \right] + \rho N_{[0, T]}.$$

If such a function V is found for a given sampling scheme, then the limit $T \rightarrow \infty$ gives the desired bounds on J_h . The objective now is twofold; to minimize \bar{J} with respect to the sampling scheme and to find a value function V such that the bounds are tight, i.e., $\underline{J} = \bar{J}$. Achieving both means that we have solved (13). The following theorem from [11, Paper II] specifies when this is the case.

Theorem 2 ([11, Paper II, Thm. 1]): Suppose a bounded \mathcal{C}^2 function $V(x_h)$ and a constant J satisfy

$$x_h^\top Q x_h + x_h^\top A^\top \nabla V + \text{Tr}(R \nabla^2 V) \geq J \quad \forall x_h \in \mathbb{R}^n, \quad (14)$$

$$\rho \geq V(x_h) - V(0) \quad \forall x_h \in \mathbb{R}^n, \quad (15)$$

where equality is achieved in either (14) or (15) for each x_h . Then the optimal cost in (13) is J and

$$\frac{1}{T}(j + \mathbb{E}[V(x_h(T)) - V(x_h(0))]) \geq J. \quad (16)$$

Equality is achieved in (16) when sampling is triggered on equality in (15), i.e., the optimal sampling scheme is

$$\phi(x_h) = \begin{cases} 1, & V(x_h) - V(0) = \rho, \\ 0, & \text{otherwise.} \end{cases}$$

Proof: See proof of Theorem 1 in [11, Paper II]. ■

Remark 2: The value function V in Theorem 2 can be seen as a measure of the expected cost per time unit at x_h . It is then optimal to sample whenever this cost exactly equals the instantaneous cost of sampling plus the expected cost at the origin, i.e., $V(x_h) = V(0) + \rho$.

The inequalities (14), (15) can also be formulated as a stationary convection–diffusion type PDE over a domain with a free boundary, a so called Stefan problem [15]. Such problems are usually found in models describing mediums undergoing phase change, e.g., melting ice.

Let Ω denote the set where equality is attained in (14). On the boundary, $\partial\Omega$, we have equality in (15), meaning that $\partial\Omega$ is a level curve of V . Since V is \mathcal{C}^2 and constant outside Ω (equality in (15)), it holds that $\nabla V = 0$ on $\partial\Omega$. We can thus write (14), (15) as

$$\begin{cases} x_h^\top Q x_h - J + x_h^\top A^\top \nabla V + \text{Tr}(R \nabla^2 V) = 0, \\ V(x_h) \leq \rho + V(0), \end{cases} \quad \forall x_h \in \mathbb{R}^n, \quad (17)$$

$$\begin{cases} V(x_h) = \rho + V(0), \\ \nabla V = 0, \end{cases} \quad \forall x_h \in \partial\Omega. \quad (18)$$

For fixed values of J , ρ , and $V(0)$, this is a Stefan problem in V with the free boundary $\partial\Omega$. The first term in (17) describes production, the second convection and the third diffusion. On the free boundary $\partial\Omega$ we have both a Dirichlet and a Neumann condition, given by (18). While PDEs of this kind in general do not have a solution in closed form, there exist several numerical solution methods, e.g., [16], [17].

B. A Closed-Form Solution for the Integrator Case

In the special case of an n -dimensional integrator, $A = 0$, there is in fact a closed-form solution to (14), (15).

Theorem 3 ([11, Paper II, Thm. 2]): For the integrator case, $A = 0$, the value function $V(x_h)$ satisfying (14) and (15) is given by

$$\begin{aligned} V(x_h) &= \begin{cases} -\frac{1}{4}g(x_h)^2, & g(x_h) \geq 0, \\ 0, & \text{otherwise,} \end{cases} \\ g(x_h) &= 2\sqrt{\rho} - x_h^\top P x_h, \end{aligned}$$

which corresponds to the optimal sampling scheme

$$\phi(x_h) = \begin{cases} 1, & 2\sqrt{\rho} - x_h^\top P x_h = 0, \\ 0, & \text{otherwise.} \end{cases}$$

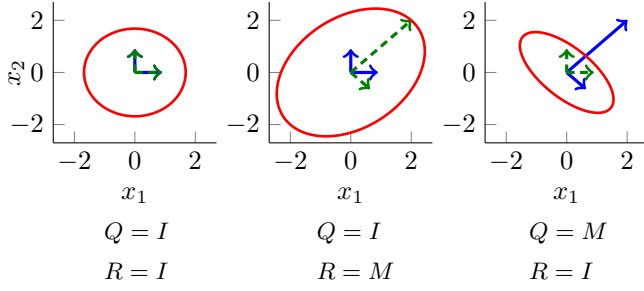


Fig. 3. Examples of the optimal, ellipsoidal, trigger bounds (red, solid) in the integrator case. The state cost matrix Q (blue, solid) and noise intensity matrix R (green, dashed) are represented by their respective eigenvectors scaled by their associated eigenvalues. For all cases $\rho = 1$ and $M = N_{\pi/4}^T \text{diag}(1, 10) N_{\pi/4}$, where N_{θ} is the rotation matrix defined in (28).

The matrix P is determined by the Riccati-like equation

$$PRP + \frac{1}{2} \text{Tr}(RP)P = Q, \quad (19)$$

which has a unique solution $P \succeq 0$ for any $R \succ 0$ and $Q \succeq 0$. The optimal cost is $J = \sqrt{\rho} \text{Tr}(RP)$, where specifically

$$\|H\|_2^2 = \rho f = \frac{1}{2} \sqrt{\rho} \text{Tr}(RP). \quad (20)$$

Proof: All statements but (20) and the uniqueness of P are proven by insertion into (14) and (15) in Theorem 2. For a detailed proof, including (20) and uniqueness of P , see [11, Paper II]. ■

The optimal trade-off between sampling rate and performance is given by the shape of the ellipsoidal trigger bound $2\sqrt{\rho} = x_H^T P x_H$, which is illustrated in Fig. 3. Directions associated with large eigenvalues of the noise intensity matrix R will typically have an out-stretched bound, sacrificing some performance to ensure fewer sampling events. The opposite is true for directions associated with large eigenvalues of the state cost matrix Q .

Using Theorems 1 and 3, we can express the performance as a function of the average sampling period $h_{\text{avg}} := 1/f$

$$\|T_{zw}\|_2^2 = \gamma_0^2 + J_e h_{\text{avg}}, \quad J_e = \frac{[\text{Tr}(RP)]^2}{4}. \quad (21)$$

With this result, it becomes interesting to compare how much optimal event-based sampling improves the performance over standard periodic sampling. The performance using periodic sampling is given by [9, Remark 4]

$$\|T_{zw}\|_2^2 = \gamma_0^2 + \frac{1}{h} \int_0^h \int_0^{h-\tau} \|D_{zu} F e^{A\sigma} L D_{yw}\|_F^2 d\sigma d\tau, \quad (22)$$

where $h = h_{\text{avg}}$ is the sampling period. With $A = 0$ we can rewrite this as

$$\|T_{zw}\|_2^2 = \gamma_0^2 + J_p h_{\text{avg}}, \quad J_p = \frac{\text{Tr}(RQ)}{2}, \quad (23)$$

by noting that $\|D_{zu} F L D_{yw}\|_F^2 = \text{Tr}(RQ)$. Based on (21), (23) we can now derive the following theorem:

Theorem 4: Using the \mathcal{H}_2 -optimal sampled-data controller structure (9), (10), the ratio of performance degradation, $J_{\text{ratio}} = J_p/J_e$, between periodic and optimal event-based sampling for the n -dimensional integrator system is bounded by

$$1 + \frac{2}{n} \leq J_{\text{ratio}} \leq 3, \quad (24)$$

with equality in the lower bound when the eigenvalues of the matrix RQ coincide, and equality in the upper bound when RQ has only one non-zero eigenvalue.

Proof: We have

$$\begin{aligned} J_{\text{ratio}} &= \frac{J_p}{J_e} = 2 \frac{\text{Tr}(RQ)}{[\text{Tr}(RP)]^2} \\ &= 2 \frac{\text{Tr}((RP)^2 + \frac{1}{2} \text{Tr}(RP)RP)}{[\text{Tr}(RP)]^2} = 2 \frac{\text{Tr}((RP)^2)}{[\text{Tr}(RP)]^2} + 1, \end{aligned}$$

where (19) was used in the third equality. Let $\lambda = [\lambda_1, \dots, \lambda_i, \dots, \lambda_n]^T$ denote the vector of eigenvalues to the matrix RP . Since $R \succ 0$ and $P \succeq 0$ we have $\lambda_i \geq 0, \forall i$. Thus $\text{Tr}(RP) = \sum_1^n \lambda_i = \sum_1^n |\lambda_i|$ and

$$J_{\text{ratio}} = 1 + 2 \frac{\text{Tr}((RP)^2)}{[\text{Tr}(RP)]^2} = 1 + 2 \frac{\|\lambda\|_2^2}{\|\lambda\|_1^2}.$$

The Cauchy–Schwarz inequality gives the vector norm bounds

$$\frac{1}{n} \leq \frac{\|\lambda\|_2^2}{\|\lambda\|_1^2} \leq 1, \quad (25)$$

which then give the bounds on J_{ratio} in (24). The lower bound in (25) is attained when all eigenvalues of RP coincide, while the upper bound is attained when RP only has one non-zero eigenvalue. To show that the same conditions are implied for the matrix RQ , we first multiply (19) with R from the left and let $RP = S J_n S^{-1}$, where J_n is the Jordan normal form of RP , and S is a similarity transform. This gives

$$S(J_n^2 + \frac{1}{2} \text{Tr}(RP)J_n)S^{-1} = RQ,$$

which means that RQ is similar to the upper triangular matrix $J_n^2 + 1/2 \text{Tr}(RP)J_n$ and shares its eigenvalues. Since these are the sum of squared and scaled eigenvalues of RP of the form $\lambda_i^2 + 1/2 \text{Tr}(RP)\lambda_i$, where $\text{Tr}(RP) \geq 0$, the conditions on RP and RQ are the same. ■

For the integrator case, the bounds (24) prove that optimal event-based sampling will always outperform periodic sampling.

C. A Numerical Method for the General Case

A closed-form solution for the general case, $A \neq 0$, still remains to be found, if it even exists. However, we have been able to obtain V numerically for the second-order case, which then by Theorem 2 also gives the optimal sampling rule.

Consider the the Stefan problem form (26), (27). Assume that we want to solve the dynamic version of the problem, for some fixed J and $V(0, t) =: -\rho, \forall t$. (The choice of

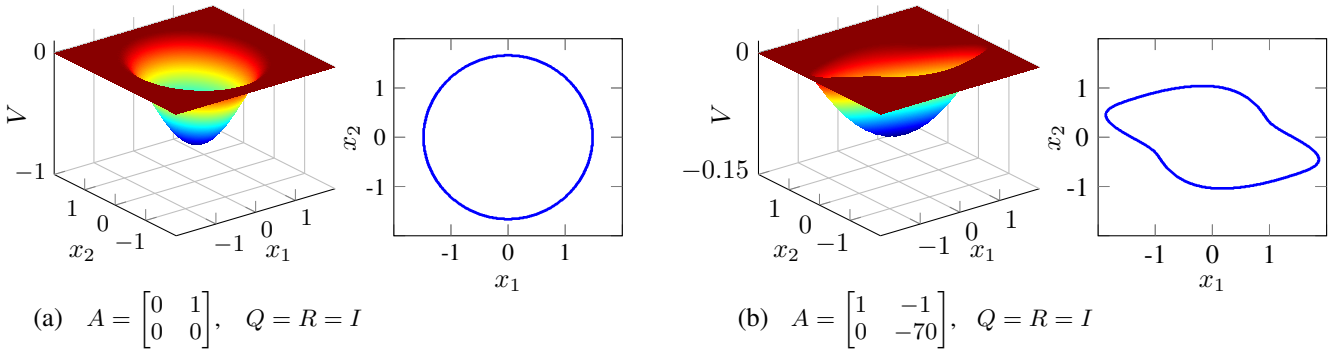


Fig. 4. Numerically obtained value function V (surface plot) and corresponding trigger bound $\partial\Omega$ (blue, solid) for (a) a double integrator system and (b) a system with dynamics of significantly different time scales. Note that the trigger bound is convex in (a) but non-convex in (b).

$V(0, t)$ is non-essential, as it only acts as a reference point for the value function). The problem is then

$$\begin{cases} x_H^\top Q x_H - J + x_H^\top A^\top \nabla V + \text{Tr}(R \nabla^2 V) = \frac{\partial V}{\partial t}, \\ V(x_H, t) \leq 0, \end{cases} \quad \forall x_H \in \mathbb{R}^n, \forall t, \quad (26)$$

$$\begin{cases} V(x_H, t) = 0, \\ \nabla V = 0, \end{cases} \quad \forall x_H \in \partial\Omega, \forall t. \quad (27)$$

The idea is to use standard numerical tools used for PDE solving to simulate (26) in discrete time, while at each time step enforcing the inequality on V . To approximate the differential operators in (26), we use the backward-time central-space (BTCS) finite difference method [18] and enforce the inequality by assigning $V := \min(V, 0)$ at each time step. This assignment has the effect of moving the free boundary $\partial\Omega$ in time. The simulation is then progressed until a stopping criterion based on stationarity of V is met. If stationarity is reached, this means that we have found a solution satisfying (17), (18) for the specific J , and thus the optimal trigger bound is given by the resulting boundary $\partial\Omega$. For further detail, we refer to the supplemental Matlab code².

The method has been validated using the known results for the case $A = 0$, and is successfully reaching a stationary solution for all second-order systems considered so far. While it in principle could be applied to higher order cases as well, it becomes unwieldy due to the computational complexity. For second-order systems, preliminary findings suggest that the trigger bound is convex and almost ellipsoidal whenever both system poles have a similar time constant. An example of this situation is seen in Fig. 4a, which shows the resulting V and trigger bound for a double (chain) integrator. However, the optimal trigger bound is not convex in general, as seen in Fig. 4b, where V and the optimal trigger bound is presented for a system with significantly different time constants.

IV. NUMERICAL EXAMPLES

Here we demonstrate the capability of the \mathcal{H}_2 -optimal controller using optimal event-based sampling through two numerical examples—one integrator and one unstable system. We compare the trade-off between performance $\|T_{zw}\|_2^2$

and average sampling period h_{avg} for four different sampled-data controller structures and sampling methods:

- (a) Standard ZOH LQG using periodic sampling.
- (b) The \mathcal{H}_2 -optimal controller structure, (9), (10), using periodic sampling.
- (c) A heuristic LQR and particle filter (PF) structure using send-on-delta (SOD) sampling [19, Sec. III.E]. The SOD scheme samples y whenever $\|y\|_2 > \delta$, where δ indirectly determines the sampling rate.
- (d) The \mathcal{H}_2 -optimal controller structure, (9), (10), using optimal event-based sampling.

A. Integrator Example

For the integrator example, $A = 0$, we consider a second-order system with the following parameters:

$$\begin{aligned} B_w &= \begin{bmatrix} (R_d^{\frac{1}{2}} N_{\pi/8})^\top & 0 \end{bmatrix}, & B_u &= I, \\ C_z &= \begin{bmatrix} Q_d^{\frac{1}{2}} N_{\pi/4} \\ 0 \end{bmatrix}, & D_{zu} &= \begin{bmatrix} 0 \\ I \end{bmatrix}, \\ C_y &= I, & D_{yw} &= \begin{bmatrix} 0 & I \end{bmatrix}, \end{aligned}$$

where

$$R_d = Q_d = \begin{bmatrix} 1 & 0 \\ 0 & 5 \end{bmatrix}, \quad N_\theta = \begin{bmatrix} \cos(\theta) & -\sin(\theta) \\ \sin(\theta) & \cos(\theta) \end{bmatrix}. \quad (28)$$

This choice of C_z and B_w corresponds to

$$Q = N_{\pi/4}^\top Q_d N_{\pi/4}, \quad R = N_{\pi/8}^\top R_d N_{\pi/8},$$

i.e., the corresponding linear reset system H will have asymmetric cost and noise intensity matrices, for which the eigenvectors are not aligned to each other, nor to the state axes. This choice ensures that the integrator states are coupled through the input noise and controlled output, as to avoid the degenerated case of two uncoupled first-order integrator processes.

To obtain trade-off curves, we use (21), (23) for (b) and (d) respectively. For (a) we use the Matlab toolbox Jitterbug [20]. Since the trade-off cannot be explicitly computed for (c), we instead simulate a sampled version of the closed-loop system with time step size $h_{\text{nom}} = 0.01$, and average the performance and sampling period over a duration of $T = 10,000$. The value h_{nom} was in this example approximately

²Available at <https://gitlab.control.lth.se/marcus/optimal-trigger-bound.git>

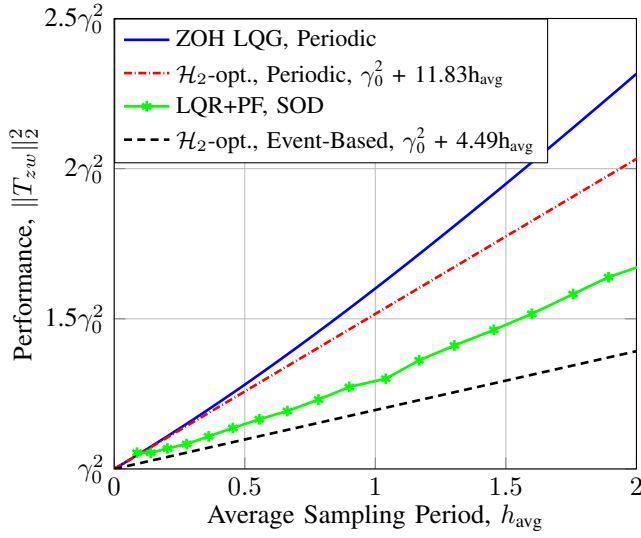


Fig. 5. Trade-off curves for performance $\|T_{zw}\|_2^2$ versus average sampling period h_{avg} for the integrator example. Here $\gamma_0^2 = 22.91$. Note that $J_{\text{ratio}} = 11.83/4.49 \approx 2.63$, falling inside the bounds $2 \leq J_{\text{ratio}} \leq 3$ from Theorem 4. The result suggests that sampling scheme, rather than controller structure, is the main performance contributor.

280 times smaller than the fastest time constant of the closed-loop system using continuous-time LQG.

The resulting trade-off curves are presented in Fig. 5. Note that the improvement made by going from the sub-optimal structure (a) to the optimal structure (b) is smaller than the improvement made by going from periodic sampling in (b) to optimal event-based sampling in (d). This suggests that sampling scheme, rather than controller structure, is the main performance contributor. This is also supported by the fact that (c) outperforms (b) by using a more efficient event-based SOD sampling scheme. The deterioration seen for (c) for small values of h_{avg} is due to the limitation of only generating events at multiples of h_{nom} in the simulation.

B. Unstable Example

For the unstable example we use the same parameters as in the previous example except for the system matrix:

$$A = \begin{bmatrix} 1 & -1 \\ 0 & -1 \end{bmatrix}.$$

For the case (d), we numerically obtain optimal trigger bounds for different values of J . The resulting trigger bounds are presented in Fig. 6. We then obtain trade-off curves for cases (c) and (d) by simulating a sampled version of the closed-loop system using $h_{\text{nom}} = 0.01$, approximately 260 times smaller than the fastest time constant of the continuous-time closed-loop LQG system. Note that (d) needs to be simulated in this example, since the average sampling period h_{avg} cannot be computed directly using V and J . We use $T = 10,000$ for the simulation of (d), but shorten the simulation time to $T = 2000$ for (c) due to particle depletion in the PF. Case (a) is still evaluated using Jitterbug, and (b) is evaluated using (22).

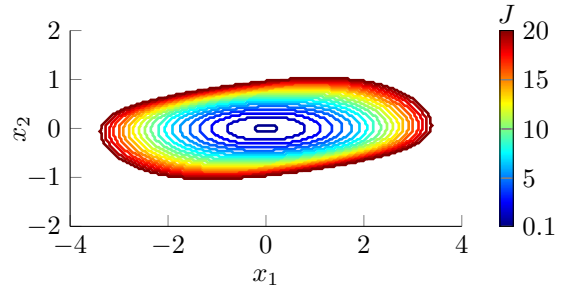


Fig. 6. Numerically obtained trigger bounds for the unstable example, here using $J \in [0.1, 20]$. Note that unlike the integrator case, the trigger bounds are not ellipses. However, they are still convex for this particular case.

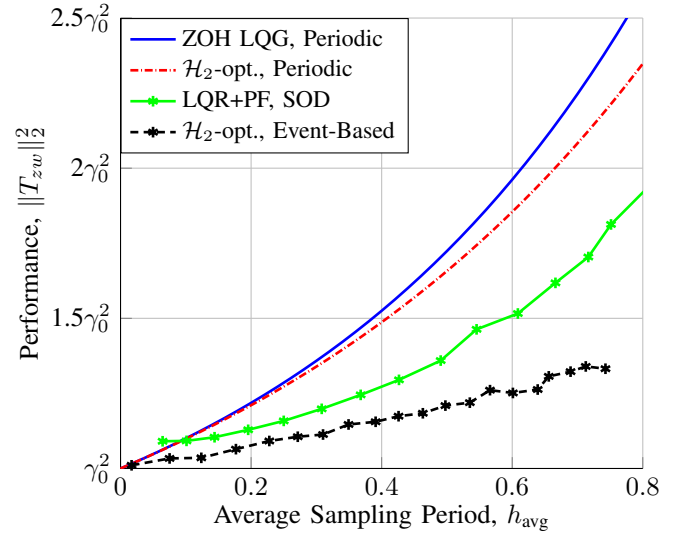


Fig. 7. Trade-off curves for performance $\|T_{zw}\|_2^2$ versus average sampling period h_{avg} for the unstable example. Here $\gamma_0^2 = 33.84$. Note that the ratio of improvement over the other controller structures grows with h_{avg} .

The resulting trade-off curves are presented in Fig. 7. This case also suggests that sampling scheme rather than controller structure is the main factor for improvement. Also note that in this example the ratio of improvement J_{ratio} is increasing with h_{avg} , whereas in the integrator example J_{ratio} was constant. This is in line with [2], [10], where similar observations were made for unstable first-order systems and unstable uncoupled second-order systems respectively.

V. CONCLUSION AND FUTURE WORK

Based on the work on optimal event-based impulse control in [11], we have presented a framework for finding the optimal event-based sampling scheme for the \mathcal{H}_2 -optimal sampled-data controller structure. The fact that the controller structure is optimal for any uniformly bounded sampling sequence implies that the resulting co-design is in fact \mathcal{H}_2 -optimal. Solving the optimization problem for the sampling scheme is equivalent to finding a value function V , satisfying a stationary PDE with free boundary. The function V , and thus the optimal sampling scheme, is available in closed form for the multidimensional integrator case. The sampling

scheme then corresponds to an ellipsoidal trigger bound in a linear reset system. Also, a numerical method has been presented for obtaining V in the second-order general case. Examples show that the trigger bound is not necessarily convex in the general case.

Future work will be focused on refining the methods of obtaining V for higher-order systems. As long as no closed-form solution is available, more efficient methods for solving the free boundary problem are required before this is a viable design method for sampled-data control synthesis. To this end it is also important to further investigate properties of the optimal trigger bound, such as uniqueness, and if it is always star shaped like in all the presented examples.

VI. ACKNOWLEDGMENTS

This work has been supported by the Swedish Research Council. The authors are members of the LCCC Linnaeus Center and the ELLIIT Excellence Center at Lund University. The authors would like to thank Toivo Henningsson and Leonid Mirkin for fruitful discussions.

REFERENCES

- [1] K. J. Åström and B. Wittenmark, *Computer-Controlled Systems (3rd Ed.)*. Upper Saddle River, NJ, USA: Prentice-Hall, Inc., 1997.
- [2] K. J. Åström and B. Bernhardsson, "Comparison of periodic and event based sampling for first-order stochastic systems," in *Proc. 14th IFAC World Congress*, vol. 11, Beijing, China, 1999, pp. 301–306.
- [3] K.-E. Årzén, "A simple event-based PID controller," in *Proc. 14th IFAC World Congress*, vol. 18, Beijing, China, 1999, pp. 423–428.
- [4] K. J. Åström, "Event Based Control," in *Analysis and Design of Nonlinear Control Systems: In Honor of Alberto Isidori*, A. Astolfi and L. Marconi, Eds. Berlin, Heidelberg: Springer, 2008, pp. 127–147.
- [5] W. P. M. H. Heemels, K. H. Johansson, and P. Tabuada, "An introduction to event-triggered and self-triggered control," in *Proc. 51st IEEE Conf. on Decision and Control*, Maui, HI, USA, 2012, pp. 3270–3285.
- [6] Q. Liu, Z. Wang, X. He, and D. Zhou, "A survey of event-based strategies on control and estimation," *Systems Science & Control Engineering*, vol. 2, no. 1, pp. 90–97, 2014.
- [7] M. Miskowicz, *Event-Based Control and Signal Processing*, ser. Embedded Systems. CRC Press, 2015.
- [8] L. Mirkin, "Intermittent redesign of analog controllers via the Youla parameter," *IEEE Trans. Automat. Control*, 2017, (to appear).
- [9] M. Braksmayer and L. Mirkin, " H_2 Optimization Under Intermittent Sampling and its Application to Event-Triggered Control," in *Proc. 20th IFAC World Congress*, Toulouse, France, 2017, accepted.
- [10] X. Meng and T. Chen, "Optimal sampling and performance comparison of periodic and event based impulse control," *IEEE Trans. Automat. Control*, vol. 57, 2012.
- [11] T. Henningsson, "Stochastic Event-Based Control and Estimation," Ph.D. dissertation, Dept. of Automatic Control, Lund University, Lund, Sweden, 2012. [Online]. Available: <http://www.control.lth.se/documents/2012/henn.t2012phd.pdf>
- [12] K. Zhou, J. C. Doyle, and K. Glover, *Robust and Optimal Control*. Prentice-Hall, Inc., 1996.
- [13] A. Goldenshluger and L. Mirkin, "On minimum-variance event-triggered control," *IEEE Control Systems Letters*, 2017, (submitted).
- [14] K. J. Åström, *Introduction to Stochastic Control Theory*, ser. Mathematics in science and engineering. Academic Press, 1970, vol. 70.
- [15] J. Stefan, "Über einige Probleme der Theorie der Wärmeleitung." *Wien. Ber.*, vol. 98, pp. 473–484, 1888.
- [16] M. K. Bernauer and R. Herzog, "Implementation of an X-FEM Solver for the Classical Two-Phase Stefan Problem," *Journal of Scientific Computing*, vol. 52, no. 2, pp. 271–293, 2012.
- [17] J. W. Barrett, H. Garcke, and R. Nürnberg, "Phase Field Models Versus Parametric Front Tracking Methods: Are They Accurate and Computationally Efficient?" *Communications in Computational Physics*, vol. 15, no. 2, p. 506555, 2014.
- [18] G. W. Recktenwald. (2011) Finite-Difference Approximations to the Heat Equation. [Online]. Available: <http://citeseerx.ist.psu.edu/viewdoc/summary?doi=10.1.1.408.4054> (Accessed 2017-03-18).
- [19] A. Cervin, "LQG-Optimal PI and PID Control as Benchmarks for Event-Based Control," in *2nd Int. Conf. on Event-based Control, Communication, and Signal Processing*, Kraków, Poland, 2016, pp. 1–8.
- [20] B. Lincoln and A. Cervin, "Jitterbug: A tool for analysis of real-time control performance," in *Proc. 41st IEEE Conference on Decision and Control*, Las Vegas, NV, USA, Dec 2002, pp. 1319–1324.